

# Identification of the unique subtype of macrophages in aneurysm lesions at the growth phase

**Akihiro Okada**

National Cerebral and Cardiovascular Center

**Hirokazu Koseki**

The Jikei University School of Medicine

**Isao Ono**

National Cerebral and Cardiovascular Center

**Tomomichi Kayahara**

National Cerebral and Cardiovascular Center

**Hiroki Kurita**

Saitama Medical University International Medical Center

**Susumu Miyamoto**

Kyoto University Graduate School of Medicine

**Hiroharu Kataoka**

National Cerebral and Cardiovascular Center

**Tomohiro Aoki** (✉ [tomoaoki@ncvc.go.jp](mailto:tomoaoki@ncvc.go.jp))

National Cerebral and Cardiovascular Center

---

## Research Article

**Keywords:** intracranial aneurysm, subarachnoid hemorrhage, macrophage, subtype, nervous system

**Posted Date:** June 23rd, 2022

**DOI:** <https://doi.org/10.21203/rs.3.rs-1756113/v1>

**License:**  This work is licensed under a Creative Commons Attribution 4.0 International License.

[Read Full License](#)

---

# Abstract

## Background

Considered with the devastating outcome of subarachnoid hemorrhage due to rupture of intracranial aneurysm (IA), a novel therapeutic strategy based on the pathogenesis of IAs should be established. Recent experimental studies have defined IAs as a macrophage-mediated chronic inflammatory disease affecting intracranial arteries. Although there are various subtypes in macrophages, what type of macrophages is present in lesions during the disease development or contributes to the pathogenesis remains to be elucidated.

## Methods

The previously-established aneurysm model of rats were used. Macrophages were labeled with the fluorescent protein, Dil, and labelled cells were isolated by a laser-microdissection method. The comprehensive gene expression profile analyses and gene ontology analyses was then done to identify a macrophage subtype present in lesions at the growth phase. The gene expression profile data from *in vitro*-differentiated bone marrow derived macrophages was acquired from the database and used as a reference data. The histopathological examinations to validate the results were also done.

## Results

The gene expression profile data of total 52 macrophages infiltrating into the lesions was acquired. The principal component analysis failed to form multiple cluster, suggesting that macrophages infiltrating in the lesions were monotonous. By comparing the profile of the macrophage subtype identified with one from *in vitro*-differentiated M0 or M1 macrophages, the macrophages in the lesions were found to be belonged to the simple and unique subtype. Because the perception of signaling from nervous system was highlighted as terms up-represented compared with terms in M0 or M1 macrophages through gene ontology analyses, the macrophage subtype in the aneurysm lesions at the growth phase might be differentiated under the influence of nervous system in the microenvironment of the disease. The histopathological examinations clarified the presence of nerves in the adventitia of intracranial artery bifurcation, supporting the above notion.

## Conclusions

The findings from the present study have provided the useful insights about the macrophage subtype in aneurysm lesions at the growth phase and also proposed this subtype or genes specifically expressed in this subtype as a therapeutic target.

# Introduction

Subarachnoid hemorrhage (SAH) due to rupture of intracranial aneurysm (IA) has a high morbidity and mortality rate, making this disease as the most severe form among stroke<sup>1,2</sup>. Considered with the devastating outcome in spite of modern technical advancement in medical interventions and medical care, a novel therapeutic strategy based on the pathogenesis of IAs should be established. Here because the observation studies have consistently revealed the positive association of the size of IAs with the annual risk of rupture<sup>3-6</sup>, the machineries mediating the growth of IAs could presumably be a target.

Recent experimental studies have successfully defined IAs as a chronic inflammatory disease affecting intracranial arteries mainly at bifurcation sites<sup>7-20</sup>. The inhibition of inflammatory responses has suppressed the initiation, the growth or the rupture of the lesions as expected<sup>10,11,16,21-23</sup>. In the process regulating the inflammation in lesions, macrophages exert the crucial role to trigger, exacerbate or maintain inflammatory responses in microenvironment of the disease<sup>7-9,13,19,20</sup>. This type of cells also functions to maintain homeostasis of tissues, regulate the pathogenesis of many inflammatory diseases or facilitate the repair of damaged tissues after the inflammation-evoked injury<sup>24-27</sup>. To exert such a various role in each microenvironment, macrophages differentiate into a suitable subtype in response to exogenous stimuli like cytokines or other factors present in situ. Thereby in microenvironment of diseases, some evoke inflammation classically known as M1-macrophage, some relief inflammation as M2-macrophage or some repair damaged tissue<sup>24-27</sup>. The presence and the ratio of each macrophage subtype thus determine the response of affected tissues. Considered with the safer and more effective therapy targeting macrophage-mediated inflammatory diseases, the suppression of a macrophage subtype exacerbating the disease and/or the activation of a subtype facilitating the relief or the repair could be an ideal strategy. In addition, the shift of macrophage differentiation to a subtype favorable via modulating microenvironment where macrophages functions may become an alternative therapeutic strategy. In this point of view, the information about macrophage subtypes infiltrating in IA lesions is still limited. Only some have reported the presence of M1- or M2-macrophages in human IA lesions and the difference in the ratio dependent of the rupture status<sup>28</sup>. However, because of the heterogeneity of cases in humans, the presence or the precise contribution of each subtype is difficult to be examined.

In the present study, we analyzed a macrophage subtype infiltrating in aneurysm lesions at the growth phase induced in rats to understand the pathogenesis more in detail and also to identify the subtype as a therapeutic target.

## Methods

### Rat aneurysm model

Seven-week-old male Sprague-Dawley rats were purchased from Japan SLC (Shizuoka, Japan). Rats were maintained on a light/dark cycle of 12 h/12 h and had free access to chow and water. Under general anesthesia by the inhalation of isoflurane (induction; 5.0 %, maintenance; 1.5~2.0 %), the left common

carotid artery (CCA) was cut in the proximal portion and moved to the right side<sup>29,30</sup>. The left CCA was then anastomosed to the right CCA in an end-to-side fashion with a 10-0 nylon suture to create a bifurcation. Hyper-volemic state was also induced by salt overloading and ligation of the left renal artery. Immediately after the above surgical manipulations, animals were fed the chow containing 8 % sodium chloride and 0.12 % 3-aminopropionitrile (Tokyo Chemical Industry, Tokyo, Japan), an inhibitor of lysyl oxidase that catalyzes the cross-linking of collagen and elastin, which facilitates degenerative changes of arterial walls.

### **Tissue transparency and immunohistochemistry**

Tissue transparency was done using paraformaldehyde-fixed specimens and CUBIC-L and CUBIC-R solutions (#T3740 or #T3741, TCI chemicals, Tokyo, Japan) as manufacturer's instructions. The images were acquired by a confocal laser microscopy (FV3000, Olympus, Tokyo, Japan).

### **Isolation of cells present in the adventitia of aneurysm walls and preparation of libraries for single cell RNA-sequencing analysis**

DiI-containing nanoparticles (Fluorescent (DiI) Control Liposomes (Neutral), #01262101, FormuMax Scientific Inc., Sunnyvale, CA) were intravenously injected in rats to label macrophages infiltrating in lesions. After 3 days, DiI-labelled macrophages were then isolated in a single-cell fashion by the laser-microdissection technique (MMI CellCut Plus, Digital Biology, Tokyo, Japan). The library for single cell RNA-sequencing analysis was prepared by an SMART-Seq Single Cell Plus Kit (#R400751, Takara Bio Inc., Shiga, Japan).

### **Single cell RNA-sequencing analysis**

Using the libraries prepared above, paired-end sequencing (2 × 75 base pair) was performed on a NextSeq500 (Illumina). Each read was then mapped to the *Rattus norvegicus* reference genome (Rnor6) using CLC genomics workbench (version 11, QIAGEN, Venlo, Netherlands). Differential expression analyses, including principal component analysis and clustering analysis, were performed using the iDEP.951 (<http://bioinformatics.sdstate.edu/idep95/>). In the analyses, gene expression profile data deposited in the data base was also used (#GSE161798 from Gene Expression Omnibus in National Center for Biotechnology Information, <https://www.ncbi.nlm.nih.gov/geo/query/acc.cgi?acc=GSE161798>).

All the raw data from RNA sequencing analysis was deposited to Gene Expression Omnibus (<https://www.ncbi.nlm.nih.gov/geo/>) (ID # Data will be deposited after the acceptance).

### **Cell culture**

HEK293 cell line and RAW264.7 cell line were maintained in Dulbecco's Modified Eagle's Medium (DMEM) (FUJIFILM Wako Pure Chemical Corporation, Osaka, Japan) supplemented with 10 % fetal bovine serum (bio sera, Nuaille, France).

Cells were treated with Dil-containing nanoparticles (Fluorescent (Dil) Control Liposomes (Neutral), #01262101, FormuMax Scientific Inc.) by adding the particles in the medium for 1 h.

## **Immunohistochemistry**

For histological analyses, animals were transcardially perfused with 4 % paraformaldehyde solution after sacrificed by the intraperitoneal administration of a lethal dose of pentobarbital sodium (200 mg/kg). The anterior cerebral artery – olfactory artery bifurcation was then harvested, and 5- $\mu$ m-thick frozen sections were prepared. In the experiments using culture cells, cells were cultured on a chamber slide (#354631, Corning, Corning, NY) and fixed by 4 % paraformaldehyde. After blocking with 3 % donkey serum (#AB\_2337258, Jackson ImmunoResearch, West Grove, PA), slices were incubated with primary antibodies followed by incubation with secondary antibodies conjugated with a fluorescence dye (Jackson ImmunoResearch). In some experiments, the primary antibody conjugated with a fluorescence dye was used. Finally, fluorescent images were acquired on a confocal fluorescence microscope system (FV3000, Olympus, Tokyo, Japan).

The antibodies used were as follows; mouse monoclonal anti-smooth muscle  $\alpha$ -actin antibody conjugated with Cy3 (#C6198, Sigma, St. Louis, MI), mouse monoclonal anti-CD68 antibody conjugated with Alexa Fluor 647 (#sc-20060AF647, Santa Cruz Biotechnology, Dallas, TX), rabbit polyclonal anti-S100 antibody (#ab66041, abcam, Cambridge, UK), mouse monoclonal anti-SOX10 antibody (#14-5923-80, Invitrogen, Carlsbad, CA) Alexa Fluor 488-conjugated donkey anti-mouse IgG H&L antibody (#A21202, Thermo Fisher Scientific, Waltham, MA), Alexa Fluor 647-conjugated donkey anti-rabbit IgG H&L antibody (#A31573, Thermo Fisher Scientific).

## **Scanning Electron Microscopy**

The specimens were fixed with 2 % paraformaldehyde and 2 % glutaraldehyde in 0.1 M sodium phosphate buffer (pH 7.4) and then stained with 1 % osmium tetroxide (Wako) in 0.1 M sodium phosphate buffer (pH 7.4). After the dehydration in a series of graded ethanol and the replacement by propylene oxide (Nacalai Tesque, Kyoto, Japan), the tissue was coated with a thin layer of platinum palladium using an ion sputter-coater (IB3, Eiko Corporation, Tokyo, Japan). Finally, images were obtained with a high-resolution scanning electron microscopy (S-4700, Hitachi High-Tech Corporation, Tokyo, Japan).

# **Results**

## **Profiling of macrophages infiltrating in the aneurysm lesions at the growth phase by single cell RNA-sequencing analyses**

The previously-established rat model of aneurysms in which lesions were induced at the surgically-created bifurcation site in a carotid artery<sup>29</sup> was used. In this model, the enlargement of aneurysm lesions occurs during 10th to 15th days after the surgical creation of bifurcation site (Fig. 1a) and this

time point is consistent among animals examined<sup>29,30</sup>. Macrophages were isolated from the lesions induced in this model on the 14th day, the time point when the lesions were estimated to be growing, by the laser-microdissection method via referencing the fluorescence, Dil, engulfed exclusively by macrophages (Fig. 1b and c, Fig. 2). The library for single cell RNA-sequencing analysis was then constructed and ones out of 52 cells isolated were successfully prepared. The RNA sequencing analyses were then done. The average mapped read count was 9830 reads per cell. Considered with the result that the profile of each cell failed to form the multiple cluster (Fig. 3a), macrophages infiltrating in aneurysm lesions during the enlargement were monotonous.

The gene expression profile of macrophages isolated from the lesions was next compared with that in other macrophage subtypes acquired from the data base (#GSE161798 from Gene Expression Omnibus in National Center for Biotechnology Information). Intriguingly, the cluster of macrophages isolated from the aneurysm lesions at the growth phase occupied the completely different area than other macrophage subtypes in the principal component analysis (Fig. 3b), suggesting the accumulation of the unique macrophage subtype. Over- or under-expressed genes are shown in the heat map, the Venn diagram (Fig. 3c and d) or tables (Tables 1 and 2, Supplementary Data Tables S1-S4).

### **Identification of the macrophage subtype present in aneurysm lesions at the growth phase**

Next, gene ontology (GO) analyses were done to characterize the macrophage subtype infiltrating in aneurysm lesions at the growth phase. When compared with gene expression profile data in bone marrow macrophages differentiated into M0 or M1 acquired from the data base (#GSE161798 from Gene Expression Omnibus in National Center for Biotechnology Information), GO terms over-represented in macrophages from the lesions included many ones related with the perception of the signaling from nervous system; most typically 'Neurotransmitter receptor activity', 'Postsynaptic neurotransmitter receptor activity', 'Neuropeptide receptor activity' or 'G protein-coupled serotonin receptor activity' in Molecular Function, 'Neuropeptide signaling pathway' or 'Serotonin receptor signaling pathway' in Biological Process and 'Integral component of postsynaptic specialization membrane', 'Postsynaptic specialization membrane' or 'GABA receptor complex' in Cellular Component (Tables 3–8). The results from GO term analyses indicates the differentiation of infiltrating macrophages into the specific and the unique macrophage subtype regulated under the alternation of nervous system in the microenvironment where aneurysm is enlarging.

GO terms under-represented in macrophages from the lesions included ones related with apoptosis, autophagy or cell cycle (Tables 9–14), indicating the reduction in cell death, engulfing activity or proliferation.

### **The presence of nerves in the adventitia of intracranial arterial walls**

To validate the potential regulation of macrophage differentiation and function in the aneurysm lesions by nervous system, the histopathological examinations were done by scanning electron microscopic observation and immunohistochemistry. The electron microscopic analyses revealed the presence of

nerve fibers along arterial walls and toward bifurcation site (Fig. 4a). The immunohistochemistry to detect Schwann cells in myelinating nerves was then done. The positive signals for S100 or Sox10, which was the marker for Schwann cells, could be detected (Fig. 4b) consistently with the results from electron microscopic analyses, confirming the presence of myelinating nerves in arterial bifurcations where IA lesions are induced.

## Discussion

Recent experimental studies have identified a variety of subtypes in macrophages and also the diverse function of each subtype in physiological or pathological conditions<sup>24-27</sup>. Because some subtypes exacerbate a disease but some relieve, the identification of a specific subset contributing to some process of a disease or a physiological phenomenon is crucial to precisely understand underlying machineries. In the present study, we thereby isolated macrophages from aneurysm lesions at the growth phase in a single-cell fashion and examined their gene expression profile by a single-cell RNA sequencing analysis to identify a subtype present in lesions. We have then identified the similar gene expression profile among macrophages infiltrated and the presence of specific and unique macrophage subtype in aneurysm lesions. In the GO term analyses, the subtype in aneurysm lesions might be determined by the stimuli from nervous system regulating arterial function in microenvironment of the lesions. The previous study enrolling over hundred thousand persons and following-up over one million person-years has supported the contribution of nervous system to the pathogenesis of IAs that high mental stress significantly increases the risk of SAH in female<sup>31</sup>. The study enrolling cases with stable coronary arterial diseases has clarified the positive correlation of the mental stress with the risk of cardiovascular events through exacerbating inflammation via IL-6 production and facilitating vagal withdrawal<sup>32</sup>. Because chronic inflammatory response has been considered as a central mediator of IA pathogenesis<sup>7,10,19,20</sup>, this study may indicate the contribution of nerve activities to the disease.

The recent experimental studies have revealed the crucial contribution of macrophages to the pathogenesis of IAs and thus successfully defined IAs as the macrophage-mediated chronic inflammatory diseases affecting intracranial arteries<sup>7,8,10,13,19</sup>. Based on the above concept, the potential of macrophage imaging as a therapeutic method to stratify IA lesions with high probability of enlargement or rupture has been demonstrated<sup>33-35</sup>. This imaging technology utilizes the engulfing ability of macrophages and thereby visualizes the presence of macrophages in lesions. This means that macrophage imaging detected every macrophage subtypes independent of their activity or function. Here, it is well-known that each macrophage subtype has a unique role in both physiological and pathological conditions, some exacerbate inflammation and tissue destruction but some relieve inflammation and facilitate tissue repair<sup>24-27</sup>. The detection of a specific subtype contributing to each stage of the pathogenesis is, therefore, more desirable. Considered with the findings from the present study and the previous one that the simple and specific macrophage subtype completely distinguished from the major macrophage subtype, M0 or M1, accumulates specifically at the enlarging region of the lesions<sup>29</sup>, the detection of this macrophage subtype may become a diagnostic modality to more precisely predict the

progression of the disease. The information about the gene expression profile acquired in the present study may become a cue.

One of the major problem about the current therapeutic strategy for IAs is the lack of medical therapy to prevent the enlargement or the rupture of unruptured IAs. As described in the previous section, macrophages function in various physiological and pathological settings via differentiating into a subtype in microenvironment in response to external stimuli like cytokine milieu, neurotransmitters from nervous system or cell-cell contact in situ. Therefore, the medical treatment targeting the specific macrophage subtype contributing to each stage of the disease is desirable to maximize the therapeutic effect and to minimize adverse effect. The information about the gene expression profile acquired in the present study could again provide a cue.

## Conclusions

Considered with the devastating outcome of SAH due to rupture of IAs, a novel therapeutic strategy based on the pathogenesis of IAs should be established. Recent experimental studies have defined IAs as a macrophage-mediated chronic inflammatory disease affecting intracranial arteries. Here, because macrophages play various role in many physiological or pathological settings via differentiating a specific subtype in response to microenvironment where they function. In the present study, the previously-established aneurysm model of rats were used and single-cell RNA sequencing analyses were done to identify a macrophage subtype in the aneurysm lesions at the growth phase. The gene expression profile data of macrophages infiltrating into lesions at the growth phase was then acquired. The principal component analysis identified the simple and unique subtype than bone marrow-differentiated M0 or M1 macrophages. The GO term analyses indicated the regulation of identified macrophage subtype by the transmitters from nervous system regulating arterial function. The findings from the present study have provided the useful insights about the macrophage subtype in aneurysm lesions at the growth phase and also the potential regulation of aneurysm pathology by nervous system.

## Abbreviations

CCA; common carotid artery

GO; gene ontology

IA; intracranial aneurysm

SAH; subarachnoid hemorrhage

## Declarations

**Ethics approval and consent to participate**

All of the following experiments, including animal care and use, complied with the National Institute of Health's Guide for the Care and Use of Laboratory Animals and complied with the National Institute of Health's Guide for the Care and Use of Laboratory Animals and were approved by the Institutional Animal Care and Use Committee of National Cerebral and Cardiovascular Center (Approval Number; #20003, #21015, #22041). The present manuscript adheres to the ARRIVE (Animal Research: Reporting of In Vivo Experiments) guidelines for reporting animal experiments.

### **Consent for publication**

Not applicable.

### **Availability of data and materials**

The datasets used and/or analyzed during the current study are available from the corresponding author on reasonable request.

### **Competing interests**

Authors declare that there are no potential competing interests.

### **Funding**

This work was supported by the Japan Agency for Medical Research and Development (AMED) (grant ID; JP20gm0810006, T.A., JP21ek0210148, H.Kataoka) , by Grant-in-Aid for Scientific Research from the Ministry of Education, Culture, Sports, Science and Technology of Japan (grant ID; 20K09381, T.A., 20K09367, H.Kataoka), and by Grant-in-Aid for Young Scientists from the Japan Society for the Promotion of Science (grant ID; 18K16599, H.Koseki, 21K16622, T.K.).

### **Author's contributions**

A. O., H. Koseki, I. O., T. K. and T. A. planned the experiments. A. O., H. Koseki, I. O., T. K. and T. A. acquired the data. A. O., H. Koseki, I. O., T. K., H. Kataoka and T. A. interpreted the data. A. O., H. Koseki, and T. A. wrote the manuscript. H. Kurita, S. M., H. Kataoka and T. A. critically reviewed and modified the manuscript. All authors read and approved the final manuscript.

### **Acknowledgements**

The authors thank the technical assistant from the Division of Electron Microscopic Study in Center for Anatomical Studies at Kyoto University Graduate School of Medicine for electron microscopy.

## **References**

1. Lawton M. T., Vates G. E.: Subarachnoid Hemorrhage. *N Engl J Med* 377:257–266, 2017.
2. van Gijn J., Kerr R. S., Rinkel G. J.: Subarachnoid haemorrhage. *Lancet* 369:306–318, 2007.

3. Morita A., Kirino T., Hashi K., et al: The natural course of unruptured cerebral aneurysms in a Japanese cohort. *N Engl J Med* 366:2474–2482, 2012.
4. Wiebers D. O., Piepgras D. G., Brown R. D., Jr., et al: Unruptured aneurysms. *J Neurosurg* 96:50–51; discussion 58–60, 2002.
5. Wermer M. J., van der Schaaf I. C., Algra A., et al: Risk of rupture of unruptured intracranial aneurysms in relation to patient and aneurysm characteristics: an updated meta-analysis. *Stroke* 38:1404–1410, 2007.
6. Greving J. P., Wermer M. J., Brown R. D., Jr., et al: Development of the PHASES score for prediction of risk of rupture of intracranial aneurysms: a pooled analysis of six prospective cohort studies. *Lancet Neurol* 13:59–66, 2014.
7. Aoki T., Frosen J., Fukuda M., et al: Prostaglandin E2-EP2-NF-kappaB signaling in macrophages as a potential therapeutic target for intracranial aneurysms. *Sci Signal* 10, 2017.
8. Aoki T., Kataoka H., Ishibashi R., et al: Impact of monocyte chemoattractant protein-1 deficiency on cerebral aneurysm formation. *Stroke* 40:942–951, 2009.
9. Aoki T., Kataoka H., Morimoto M., et al: Macrophage-derived matrix metalloproteinase-2 and -9 promote the progression of cerebral aneurysms in rats. *Stroke* 38:162–169, 2007.
10. Aoki T., Kataoka H., Shimamura M., et al: NF-kappaB is a key mediator of cerebral aneurysm formation. *Circulation* 116:2830–2840, 2007.
11. Aoki T., Nishimura M., Matsuoka T., et al: PGE(2) -EP(2) signalling in endothelium is activated by haemodynamic stress and induces cerebral aneurysm through an amplifying loop via NF-kappaB. *Br J Pharmacol* 163:1237–1249, 2011.
12. Fukuda S., Hashimoto N., Naritomi H., et al: Prevention of rat cerebral aneurysm formation by inhibition of nitric oxide synthase. *Circulation* 101:2532–2538, 2000.
13. Kanematsu Y., Kanematsu M., Kurihara C., et al: Critical roles of macrophages in the formation of intracranial aneurysm. *Stroke* 42:173–178, 2011.
14. Koseki H., Miyata H., Shimo S., et al: Two Diverse Hemodynamic Forces, a Mechanical Stretch and a High Wall Shear Stress, Determine Intracranial Aneurysm Formation. *Transl Stroke Res* 11:80–92, 2020.
15. Kushamae M., Miyata H., Shirai M., et al: Involvement of neutrophils in machineries underlying the rupture of intracranial aneurysms in rats. *Sci Rep* 10:20004, 2020.
16. Yokoi T., Isono T., Saitoh M., et al: Suppression of cerebral aneurysm formation in rats by a tumor necrosis factor-alpha inhibitor. *J Neurosurg* 120:1193–1200, 2014.
17. Starke R. M., Chalouhi N., Jabbour P. M., et al: Critical role of TNF-alpha in cerebral aneurysm formation and progression to rupture. *J Neuroinflammation* 11:77, 2014.
18. Aoki T., Fukuda M., Nishimura M., et al: Critical role of TNF-alpha-TNFR1 signaling in intracranial aneurysm formation. *Acta Neuropathol Commun* 2:34, 2014.

19. Shimizu K., Kushamae M., Mizutani T., et al: Intracranial Aneurysm as a Macrophage-mediated Inflammatory Disease. *Neurol Med Chir (Tokyo)* 59:126–132, 2019.
20. Frosen J., Cebal J., Robertson A. M., et al: Flow-induced, inflammation-mediated arterial wall remodeling in the formation and progression of intracranial aneurysms. *Neurosurg Focus* 47:E21, 2019.
21. Aoki T., Kataoka H., Ishibashi R., et al: Pitavastatin suppresses formation and progression of cerebral aneurysms through inhibition of the nuclear factor kappaB pathway. *Neurosurgery* 64:357–365; discussion 365 – 356, 2009.
22. Aoki T., Kataoka H., Ishibashi R., et al: Simvastatin suppresses the progression of experimentally induced cerebral aneurysms in rats. *Stroke* 39:1276–1285, 2008.
23. Yamamoto R., Aoki T., Koseki H., et al: A sphingosine-1-phosphate receptor type 1 agonist, ASP4058, suppresses intracranial aneurysm through promoting endothelial integrity and blocking macrophage transmigration. *Br J Pharmacol* 174:2085–2101, 2017.
24. Chinetti-Gbaguidi G., Colin S., Staels B.: Macrophage subsets in atherosclerosis. *Nat Rev Cardiol* 12:10–17, 2015.
25. Jinnouchi H., Guo L., Sakamoto A., et al: Diversity of macrophage phenotypes and responses in atherosclerosis. *Cell Mol Life Sci* 77:1919–1932, 2020.
26. Mantovani A., Biswas S. K., Galdiero M. R., et al: Macrophage plasticity and polarization in tissue repair and remodelling. *J Pathol* 229:176–185, 2013.
27. Mosser D. M., Edwards J. P.: Exploring the full spectrum of macrophage activation. *Nat Rev Immunol* 8:958–969, 2008.
28. Hasan D., Chalouhi N., Jabbour P., et al: Macrophage imbalance (M1 vs. M2) and upregulation of mast cells in wall of ruptured human cerebral aneurysms: preliminary results. *J Neuroinflammation* 9:222, 2012.
29. Shimizu K., Kataoka H., Imai H., et al: Hemodynamic Force as a Potential Regulator of Inflammation-Mediated Focal Growth of Saccular Aneurysms in a Rat Model. *J Neuropathol Exp Neurol* 80:79–88, 2021.
30. Shimizu K., Imai H., Kawashima A., et al: Induction of CCN1 in Growing Saccular Aneurysms: A Potential Marker Predicting Unstable Lesions. *J Neuropathol Exp Neurol* 80:695–704, 2021.
31. Yamada S., Koizumi A., Iso H., et al: Risk factors for fatal subarachnoid hemorrhage: the Japan Collaborative Cohort Study. *Stroke* 34:2781–2787, 2003.
32. Moazzami K., Wittbrodt M. T., Lima B. B., et al: Higher Activation of the Rostromedial Prefrontal Cortex During Mental Stress Predicts Major Cardiovascular Disease Events in Individuals With Coronary Artery Disease. *Circulation* 142:455–465, 2020.
33. Aoki Tomohiro, Saito Makoto, Koseki Hirokazu, et al: Macrophage imaging of cerebral aneurysms with ferumoxytol: an exploratory study in an animal model and in patients. *Journal of Stroke and Cerebrovascular Disease*, 2016.

34. Hasan D. M., Mahaney K. B., Magnotta V. A., et al: Macrophage imaging within human cerebral aneurysms wall using ferumoxytol-enhanced MRI: a pilot study. *Arterioscler Thromb Vasc Biol* 32:1032–1038, 2012.
35. Shimizu K., Kushamae M., Aoki T.: Macrophage Imaging of Intracranial Aneurysms. *Neurol Med Chir (Tokyo)* 59:257–263, 2019.

## Tables

Tables 1 to 14 are available in the Supplementary Files section.

## Figures

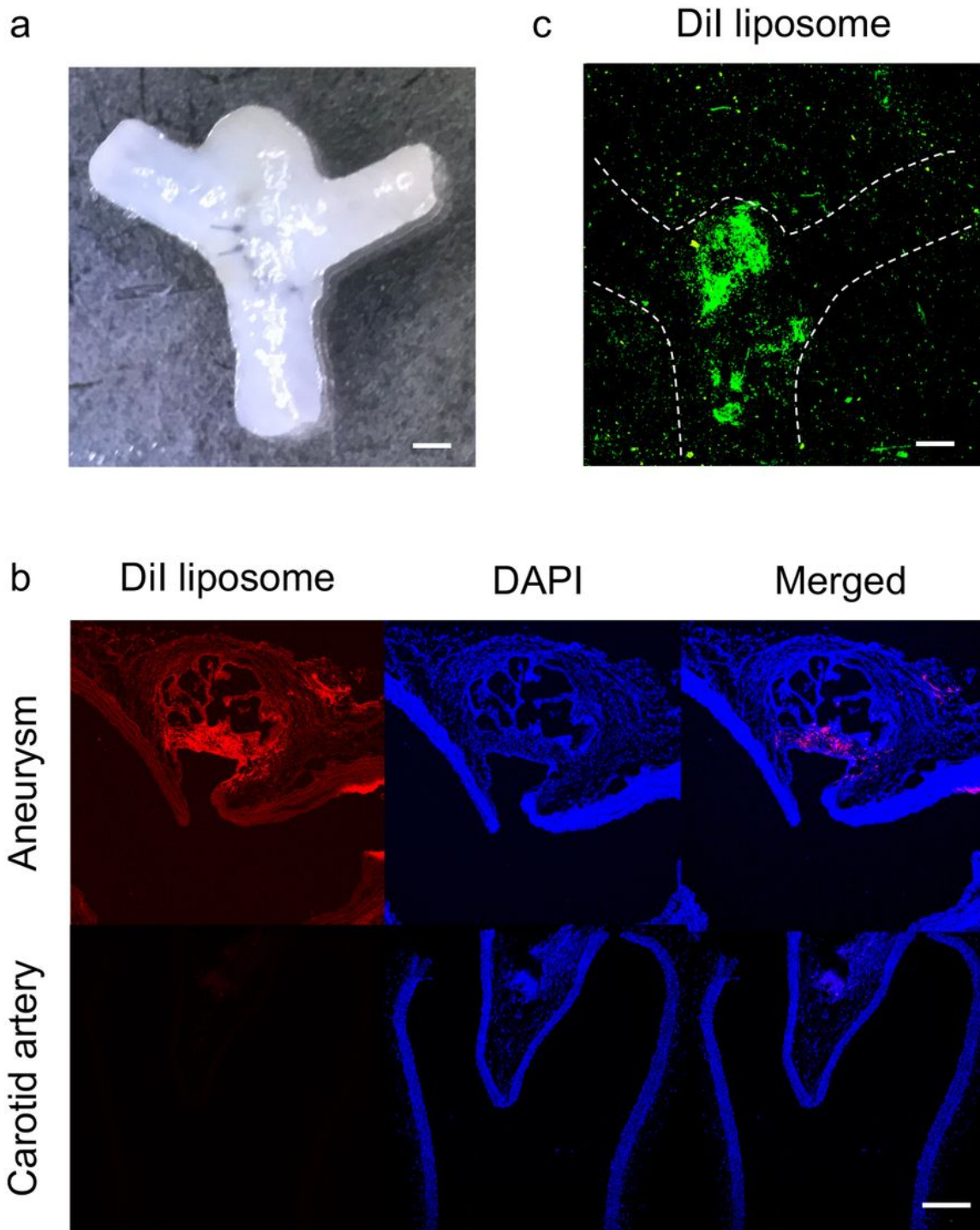


Figure 1

**The labeling of macrophages accumulating in aneurysm lesions in rats.**

The labeling of macrophages accumulating in aneurysm lesions induced in the surgically-formed bifurcation site induced in carotid artery of rats. The macrophages accumulating in the surgically-formed bifurcation site induced in carotid artery of rats is shown (a). The macrophages

were labeled by the engulfment of liposome containing fluorescent protein, Dil, were then visualized. The representative images of accumulating macrophages in lesions from sections (b) or specimens with tissue transparency (c) are shown. Scale Bars in (a), (b) or (c); 400  $\mu$ m, 200  $\mu$ m or 400  $\mu$ m.

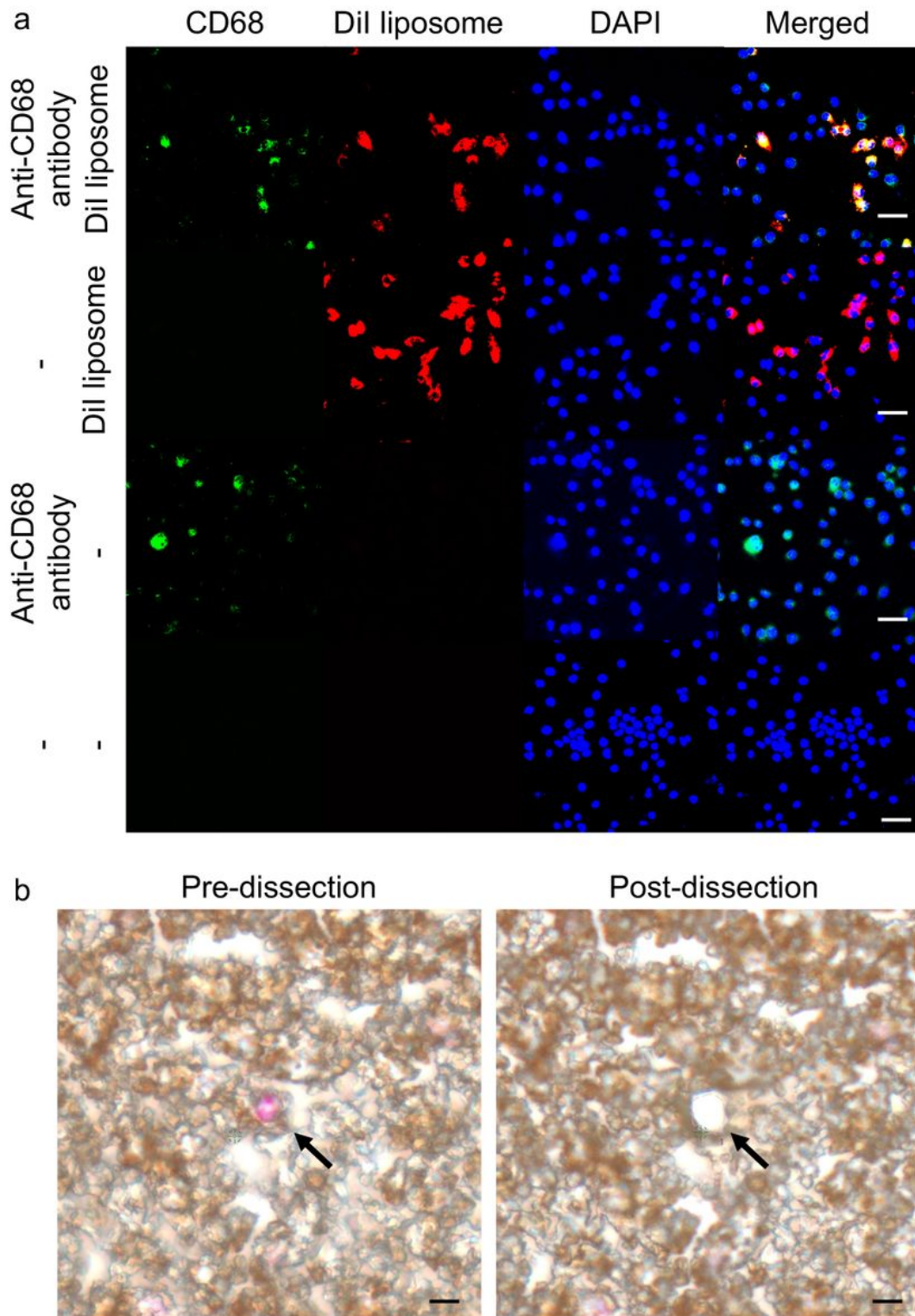


Figure 2

## **Engulfing of Dil-containing liposome specifically by macrophages and the dissection of macrophages by referencing Dil.**

(a) Engulfing of Dil-containing liposome specifically by macrophages. HEK293 cells and RAW264.7 cells were co-cultured and treated with Dil-containing liposome subjecting to immunohistochemistry. The images from immunohistochemistry for the macrophage marker, CD68 (green), the images of Dil (red), the nuclear staining by DAPI (blue) or the merged images are shown. Scale bar; 50  $\mu\text{m}$ . (b) The dissection of macrophages by laser-microdissection technique. Macrophages were isolated by laser-microdissection technique by referencing Dil. The images before or after the dissection are shown. Scale bar; 10  $\mu\text{m}$ .

### **Figure 3**

#### **The identification of the unique macrophage subtype in aneurysm lesions at the growth phase.**

(a) The clustering analysis for gene expression profile in macrophages isolated from aneurysm lesions at the growth phase. (b) The principal component analysis of gene expression profile in macrophages isolated from aneurysm lesions, bone-marrow derived M0 macrophages or M1 macrophages. (c, d) The heat map and the Venn diagram of over-expressed (c) or under-expressed genes (d) in macrophages isolated from aneurysm lesions compared with that in bone-marrow derived M0 macrophages or M1 macrophages.

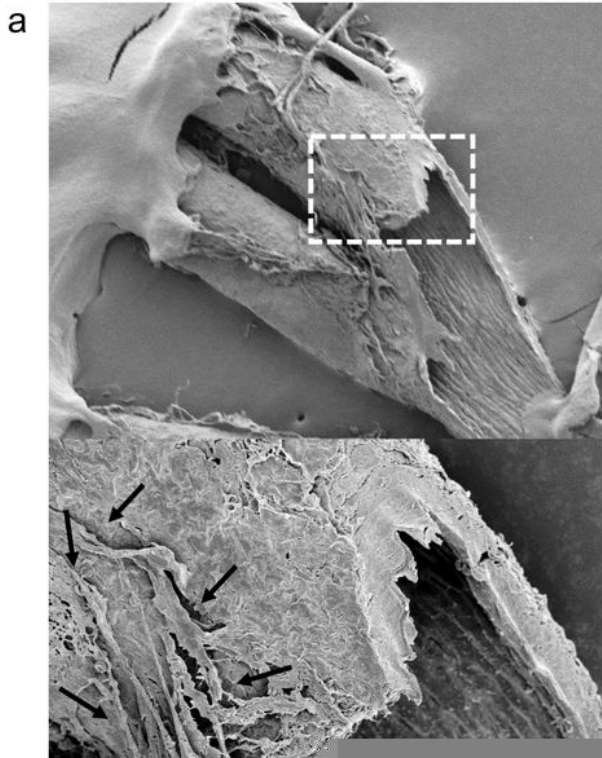


**Figure 4**

**The presence of nerves along arterial walls in bifurcation of intracranial arteries.**

The presence of myelinating nerves along arterial walls at bifurcation sites. The bifurcation site of anterior cerebral artery – olfactory artery was harvested subjecting to scanning electron microscopic examination and immunohistochemistry. The images from the scanning electron microscopic

examination (a) and the immunohistochemistry for the smooth muscle cell marker,  $\alpha$ -smooth muscle actin (red in b), the markers for Schwann cells, S100 (gray in b) or Sox10 (green in b), and merged image with nuclear staining by DAPI (blue in b) are shown (b). The magnified image corresponding to the square in the upper panel is shown in the lower panel in (a). Scale bar; 50  $\mu$ m.

## Supplementary Files

This is a list of supplementary files associated with this preprint. Click to download.

- [SupplementaryDataTableS1.xlsx](#)
- [SupplementaryDataTableS2.xlsx](#)
- [SupplementaryDataTableS3.xlsx](#)
- [SupplementaryDataTableS4.xlsx](#)
- [Table1.xlsx](#)
- [Table2.xlsx](#)
- [Table3.xlsx](#)
- [Table4.xlsx](#)
- [Table5.xlsx](#)
- [Table6.xlsx](#)
- [Table7.xlsx](#)
- [Table8.xlsx](#)
- [Table9.xlsx](#)
- [Table10.xlsx](#)
- [Table11.xlsx](#)
- [Table12.xlsx](#)
- [Table13.xlsx](#)
- [Table14.xlsx](#)